Histone deacetylase inhibition mitigates fibrosis-driven disease progression in recessive dystrophic epidermolysis bullosa

Alessia Primerano,[1] Emanuela De Domenico,[1] Francesca Cianfarani,[1] Naomi De Luca,[1] Giovanna Floriddia,[1] Massimo Teson,[1] Cristina Cristofoletti,[2] Silvia Cardarelli,[3] Giovanni Luca Scaglione,[1] Enke Baldini,[3] Davide Cangelosi,[4] Paolo Uva,[4] Jonathan Fernando Reinoso Sánchez,[1] Carole Roubaty,[5] Jörn Dengjel,[5] Alexander Nyström,[6] Simona Mastroeni,[7] Salvatore Ulisse,[3] Daniele Castiglia[1] and Teresa Odorisio[1]

[1]Laboratory of Molecular and Cell Biology, IDI-IRCCS, Rome, Italy
[2]Laboratory of Molecular Oncology, IDI-IRCCS, Rome, Italy
[3]Laboratory of Experimental Medicine, Department of Surgery, Sapienza University, Rome, Italy
[4]Clinical Bioinformatics, IRCCS Istituto Giannina Gaslini, Genoa, Italy
[5]Department of Biology, University of Fribourg, Fribourg, Switzerland
[6]Department of Dermatology, University of Freiburg, Freiburg, Germany
[7]Clinical Epidemiology Unit, IDI-IRCCS, Rome, Italy

A.P., E.D.D. and F.C. contributed equally to this paper.

Correspondence: Teresa Odorisio. Email: t.odorisio@idi.it

Linked Article: South *Br J Dermatol* 2024; **191**:482–483.

Abstract

Background Recessive dystrophic epidermolysis bullosa (RDEB) is a blistering disease caused by mutations in the gene encoding type VII collagen (C7). RDEB is associated with fibrosis, which is responsible for severe complications. The phenotypic variability observed in siblings with RDEB suggests that epigenetic modifications contribute to disease severity. Identifying epigenetic changes may help to uncover molecular mechanisms underlying RDEB pathogenesis and new therapeutic targets.

Objectives To investigate histone acetylation in RDEB skin and to explore histone deacetylase inhibitors (HDACi) as therapeutic molecules capable of counteracting fibrosis and disease progression in RDEB mice.

Methods Acetylated histone levels were detected in human skin by immunofluorescence and in RDEB fibroblasts by enzyme-linked immunosorbent assay (ELISA). The effects of givinostat and valproic acid (VPA) on RDEB fibroblast fibrotic behaviour were assessed by a collagen–gel contraction assay, Western blot and immunocytofluorescence for α-smooth muscle actin, and ELISA for released transforming growth factor (TGF)-β1. RNA sequencing was performed in HDACi- and vehicle-treated RDEB fibroblasts. VPA was systemically administered to RDEB mice and effects on overt phenotype were monitored. Fibrosis was investigated in the skin using histological and immunofluorescence analyses. Eye and tongue defects were examined microscopically. Mass spectrometry proteomics was performed on skin protein extracts from VPA-treated RDEB and control mice.
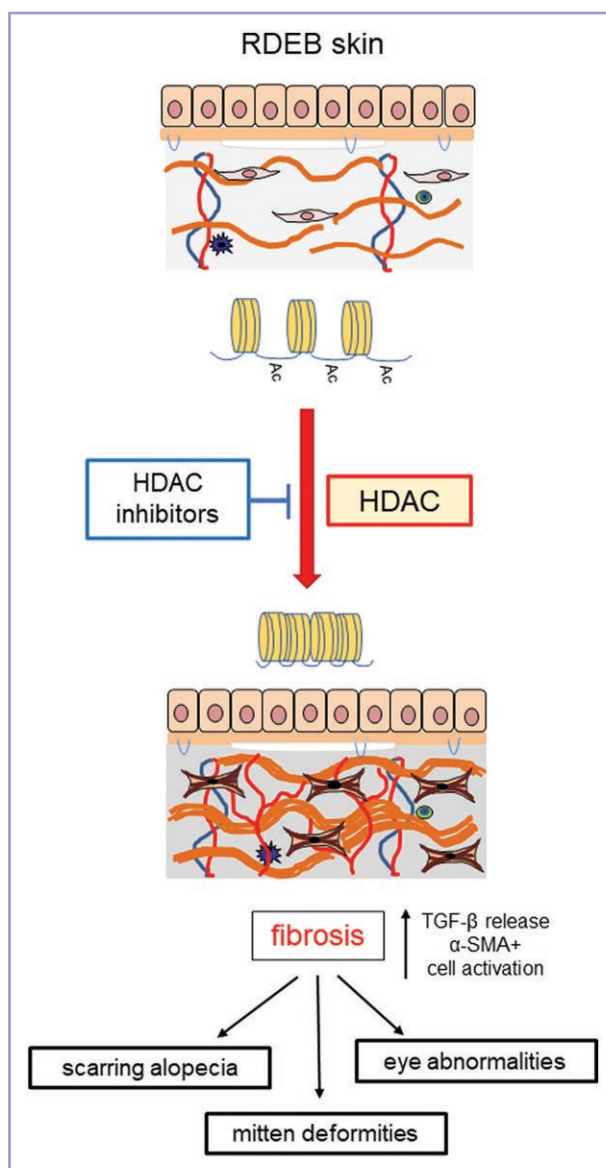
Results Histone acetylation decreases in RDEB skin and primary fibroblasts. RDEB fibroblasts treated with HDACi lowered fibrotic traits, including contractility, TGF-β1 release and proliferation. VPA administration to RDEB mice mitigated severe manifestations affecting the eyes and paws. These effects were associated with fibrosis inhibition. Proteomic analysis of mouse skin revealed that VPA almost normalized protein sets involved in protein synthesis and immune response, processes linked to the increased susceptibility to cancer and bacterial infections seen in people with RDEB.

Conclusions Dysregulated histone acetylation contributes to RDEB pathogenesis by facilitating the progression of fibrosis. Repurposing of HDACi could be considered for disease-modifying treatments in RDEB.

Graphical Abstract

Lay summary

Recessive dystrophic epidermolysis bullosa (or 'RDEB') is a rare skin disease that affects fewer than 5,000 people in the USA. A similar number of people in Europe are affected. RDEB is caused by mutations in the gene that controls the production of a protein called 'type VII collagen' (or 'C7'). A shortage of C7 causes fragile skin that blisters. In severe forms of RDEB, wounds heal slowly and can even affect a person's life expectancy. Differences in the disease are common in people (even identical twins) with RDEB who have similar levels of C7. This suggests that how severe the disease is could be affected by molecular processes that control other genes. Understanding these processes may help us to find treatments for RDEB.

This study was done in Italy, in collaboration with centres in Germany and Switzerland. We wanted to see whether a chemical modification called 'histone acetylation' (which influences gene activity) is different in RDEB and whether it can be targeted by a specific treatment.

We found that histone acetylation is reduced in RDEB skin and in skin cells grown in the lab called 'fibroblasts'. When we increased histone acetylation in fibroblasts with two drugs called givinostat and valproic acid, the amount of scar tissue produced decreased. This is important because scar tissue can lead to severe symptoms. We carried out more experiments to study the effects of givinostat and valproic acid in mice with RDEB. We found that valproic acid reduces the severity of RDEB by decreasing the disease's harmful effects and reducing the amount of scar tissue.

Our findings suggest that abnormal histone acetylation contributes to the scar tissue seen in RDEB. Our study shows that valproic acid could be useful in treating the scarring seen in RDEB and in reducing the effects of the disease. As this drug is used to treat other diseases, there could be potential for rapid repurposing of it for RDEB.

What is already known about this topic?

- Transforming growth factor (TGF)-β-driven fibrosis accounts for the development of severe secondary disease manifestations in recessive dystrophic epidermolysis bullosa (RDEB).
- Combating fibrosis is a subject of interest for the treatment of RDEB.
- Histone acetylation and epigenetic modulators have been identified as potential therapeutics for fibrosis in other disorders.

What does this study add?

- Histone acetylation levels are decreased in the skin and fibroblasts of people with RDEB.
- These levels can be modulated in fibroblasts by treatment with histone deacetylase inhibitors (HDACi), resulting in a moderation of fibrotic cell features.
- The HDACi valproic acid counteracts disease progression in an RDEB mouse model.

What is the translational message?

- Our findings provide evidence that a type of histone modification is altered in RDEB skin and may contribute to the modification of RDEB disease severity and course.
- Histone acetylation can be targeted by epigenetic modulators, which may be of significant relevance in symptom-relief treatments for RDEB.
- Valproic acid is approved and widely used for neurological disorders; therefore, it could be rapidly repurposed for the treatment of RDEB.

Recessive dystrophic epidermolysis bullosa (RDEB) is a skin and mucous membrane blistering disease caused by biallelic mutations in the *COL7A1* gene, which encodes type VII collagen (C7).[1] C7 is the major component of anchoring fibrils – structures that ensure the firm adhesion of stratified epithelia to mesenchyme.[2] Defective C7 causes unremitting blistering and impairs wound healing.[3,4] These effects, combined with prolonged inflammation, promote fibrosis, which leads to severe secondary systemic manifestations.[2,5]

Transforming growth factor-β1 (TGF-β1) has been implicated in RDEB fibrosis.[6,7] Loss of C7 results in disruption of dermal protein homeostasis, which may be associated with altered TGF-β1 bioavailability.[2,8,9] TGF-β1 induces the differentiation of progenitor cells into myofibroblasts – contractile cells that release large amounts of extracellular matrix (ECM).[10] Myofibroblasts contribute to wound contraction and ECM deposition and then undergo apoptosis.[11] RDEB skin is populated with apoptosis-resistant myofibroblasts that help maintain a fibrotic environment by releasing a high amount of TGF-β1.[7]

Gene-, protein- and cell-based therapies aimed at increasing C7 levels have been developed;[12,13] however, efficacy and safety issues, as well as costs, are limitations. A topical gene therapy using a nonreplicating herpesvirus vector has recently been approved for wound treatment.[14,15] Despite this clinical achievement, a topical approach is not ideal for a disease with systemic consequences; moreover, the episomic nature of the vector does not allow for permanent C7 expression. In this scenario, the development of approaches aimed at counteracting fibrosis and its consequences might represent a therapeutic option. Two antifibrosis biomolecules – losartan and decorin – have shown promising results at a preclinical level,[16,17] and have been selected for human therapy in RDEB (EudraCT: 2015-003670-32; https://www.debra.org.uk/decorin-gel-to-reduce-scarring).

Reduced histone acetylation due to histone deacetylase (HDAC) hyperactivity is an epigenetic mark of tissue fibrosis.[18,19] Eighteen HDACs have been identified: 11 are zinc-dependent and 7 (known as sirtuins) are nicotinamide adenine dinucleotide-dependent enzymes.[20] HDACs remove acetyl groups from histone lysine residues, promoting chromatin compaction and repressing transcription. By enhancing chromatin relaxation, HDAC inhibitors (HDACi) promote the transcription of genes with direct or indirect antifibrotic effects.[21,22] Notably, the phenotypic concordance is low in families affected by RDEB, suggesting a role of epigenetic changes in modifying disease manifestations.[7,23–25]

In this study, histone acetylation levels were analysed in skin and cultured fibroblasts from people with RDEB and compared with unaffected controls. The antifibrotic ability of valproic acid (VPA) and givinostat (ITF2357) – two HDACi that act on multiple zinc-dependent HDACs (pan-HDACi) – was tested in RDEB fibroblasts and in an RDEB mouse model.[26] Givinostat is a hydroxamate in a phase III clinical trial for Duchenne muscular dystrophy (https://www.clinicaltrials.gov/study/NCT02851797) and VPA is a short-chain fatty acid, widely used to treat neurological disorders.

Materials and methods

Patients

Skin biopsies and primary fibroblasts were obtained from people with and without RDEB (Tables S1, S2; see

Supporting Information). Patients with RDEB were diagnosed by clinical criteria, immunofluorescence antigen mapping and *COL7A1* mutation screening.

Statistical analysis

The numerical results are presented as mean (SD) unless otherwise stated. When comparing two experimental groups, an unpaired two-tailed Student's *t*-test was performed after checking the data for normality distribution using the D'Agostino–Pearson test; otherwise, a nonparametric Mann–Whitney *U* test was used. For three experimental groups, the ordinary one-way ANOVA test of variance followed by Dunnett's or Tukey's multiple comparison test was used. Prism version 8.4.3 (GraphPad, San Diego, CA, USA) was used for statistical analyses. Additional Materials and methods may be found in the Supporting Information on the journal website.
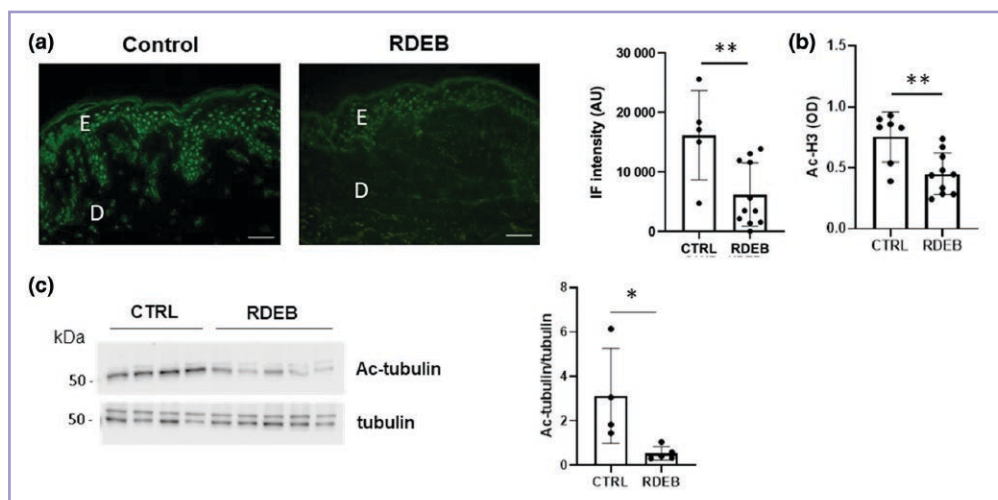
Results

Histone acetylation is reduced in skin and cultured fibroblasts of people with recessive dystrophic epidermolysis bullosa

Immunofluorescence for acetylated histone 3 (Ac-H3) was performed on RDEB ($n = 11$) and non-RDEB ($n = 5$) skin samples (Figure 1a). Fluorescence intensity was lower in RDEB skin samples. A reduction in Ac-H3 levels was confirmed by enzyme-linked immunosorbent assay (ELISA) in protein extracts of primary fibroblasts taken from people with ($n = 10$) and without ($n = 7$) RDEB (Figure 1b). Western blot analysis revealed decreased levels of acetylated tubulin in RDEB fibroblasts vs. non-RDEB cells (Figure 1c), suggesting that global acetylation activity is affected in RDEB skin.

Histone deacetylase inhibition counteracts the fibrotic phenotype of recessive dystrophic epidermolysis bullosa fibroblasts

Cultured RDEB fibroblasts resemble myofibroblasts as they release high levels of TGF-β1, express α-smooth muscle actin (α-SMA) and strongly contract a collagen gel. To test whether HDAC activity contributes to the profibrotic behaviour of RDEB fibroblasts, these cells were treated with two pan-HDACi – givinostat (ITF2357) and VPA – after defining the drug concentration and time of administration in preliminary experiments (Figure S1; see Supporting Information). RDEB fibroblasts were treated with 250 nmol L⁻¹ givinostat or 2 mmol L⁻¹ VPA for 72 h and then seeded in collagen for contractility assays ($n = 5$; Figure 2a). Both HDACi exhibited an inhibitory effect on gel contraction at 8 h, which became increasingly more evident up to 48 h. α-SMA expression – assessed by Western blot on proteins extracted from collagen gels – was significantly reduced in four of the five RDEB primary fibroblast cultures (Figure 2b), whereas it did not change in cells from treated patient #13, which showed very low α-SMA expression in the pretreatment condition (Figure S2; see Supporting Information). The α-SMA expression data were confirmed by immunofluorescence on fibroblasts treated with HDACi for 72 h (Figure 2c). Released TGF-β1 was significantly reduced in collagen lattice supernatants following treatment with givinostat or VPA (Figure 2d).

The release of inflammatory cytokines/chemokines was assessed by ELISA in lattice supernatants. Panels containing interleukin (IL)-1α, IL-1β, IL-6, IL-7, IL-8, IL-17A, interferon-γ, tumour necrosis factor (TNF)-α, vascular endothelial growth factor (VEGF)-A, CCL2 (monocyte chemoattractant protein-1) and CCL7 (MCP-3) were analysed as most are involved in RDEB chronic inflammation (Figure 2e).[4,7,27] Among the molecules found at detectable levels, IL-6 increased and VEGF-A decreased following givinostat and

Figure 1 Reduced histone acetylation in recessive dystrophic epidermolysis bullosa (RDEB) skin and primary fibroblasts. (a) Representative immunofluorescence (IF) staining for acetylated histone 3 (Ac-H3) on cryopreserved skin from a healthy control and a patient with RDEB. Nuclear staining is weaker in the nuclei of the RDEB sample in the epidermis (E) and within the dermis (D). Scale bars = 30 µm. (Right) Histogram with values obtained by analysing fluorescence intensity in skin samples from people with RDEB and healthy donors. (b) Enzyme-linked immunosorbent assay for Ac-H3 in protein extracts of fibroblasts from people with RDEB and healthy controls. (c) Western blot for acetylated (Ac) tubulin and total tubulin, used as loading control, on proteins extracted from fibroblasts from healthy donors (CTRL) or from people with RDEB. (Right) Histogram showing values of Ac-tubulin band intensity vs. total tubulin. *$P < 0.05$; **$P < 0.01$. AU, arbitrary unit; OD, optical density.

VPA treatment, while IL-8 and CCL7 were increased only after VPA administration.
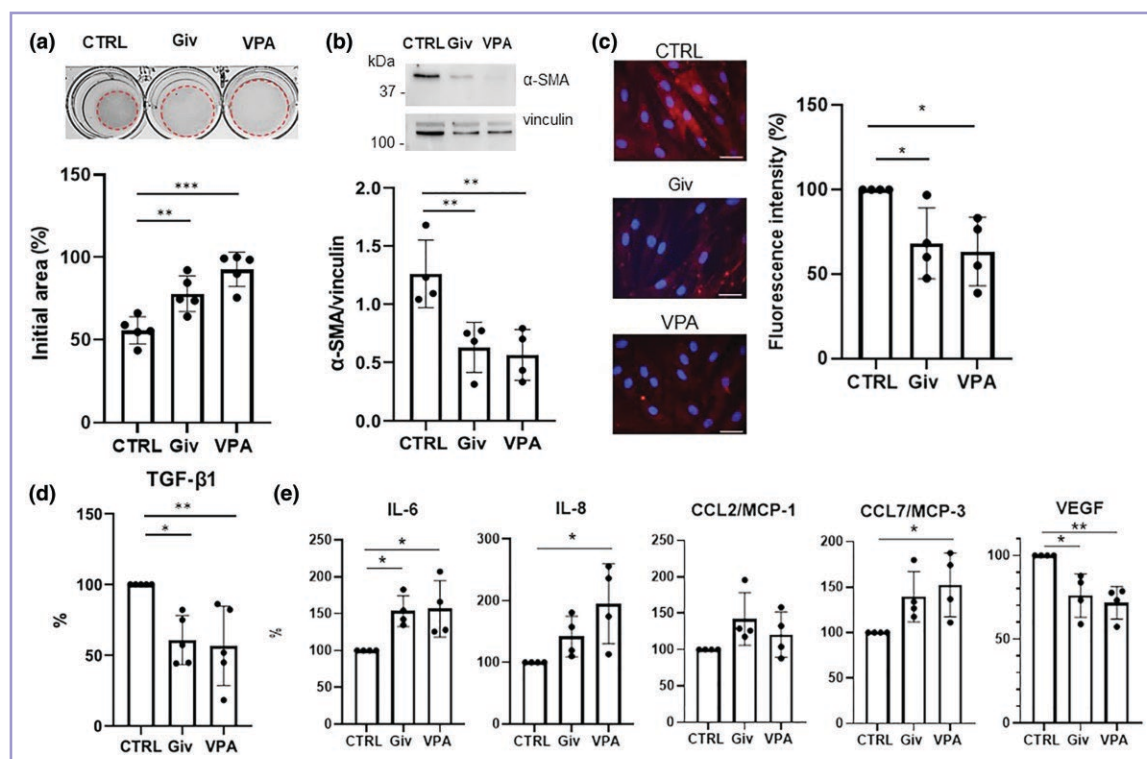
Givinostat and sodium valproate transcriptional effects on recessive dystrophic epidermolysis bullosa fibroblasts

To characterize the effects of HDACi treatment on RDEB fibroblasts at the molecular level, RNA sequencing (RNA-Seq) analysis was performed on cells treated for 30 h. This timepoint was chosen based on the recovery of H3 acetylation levels observed by ELISA after 24 h and 48 h of treatment (Figure S3; see Supporting Information).

Principal component analysis showed a separation between HDACi-treated samples and vehicle-treated ones, and that samples from the same patient treated with givinostat or VPA were proximate within the plot, indicating that the two pan-HDACi had similar effects on the gene expression profile (Figure 3a). A subset of genes was upregulated ($n = 965/1619$; 59.6%) or downregulated ($n = 225/663$; 33.9%) by both givinostat and VPA (Figure 3b, c).
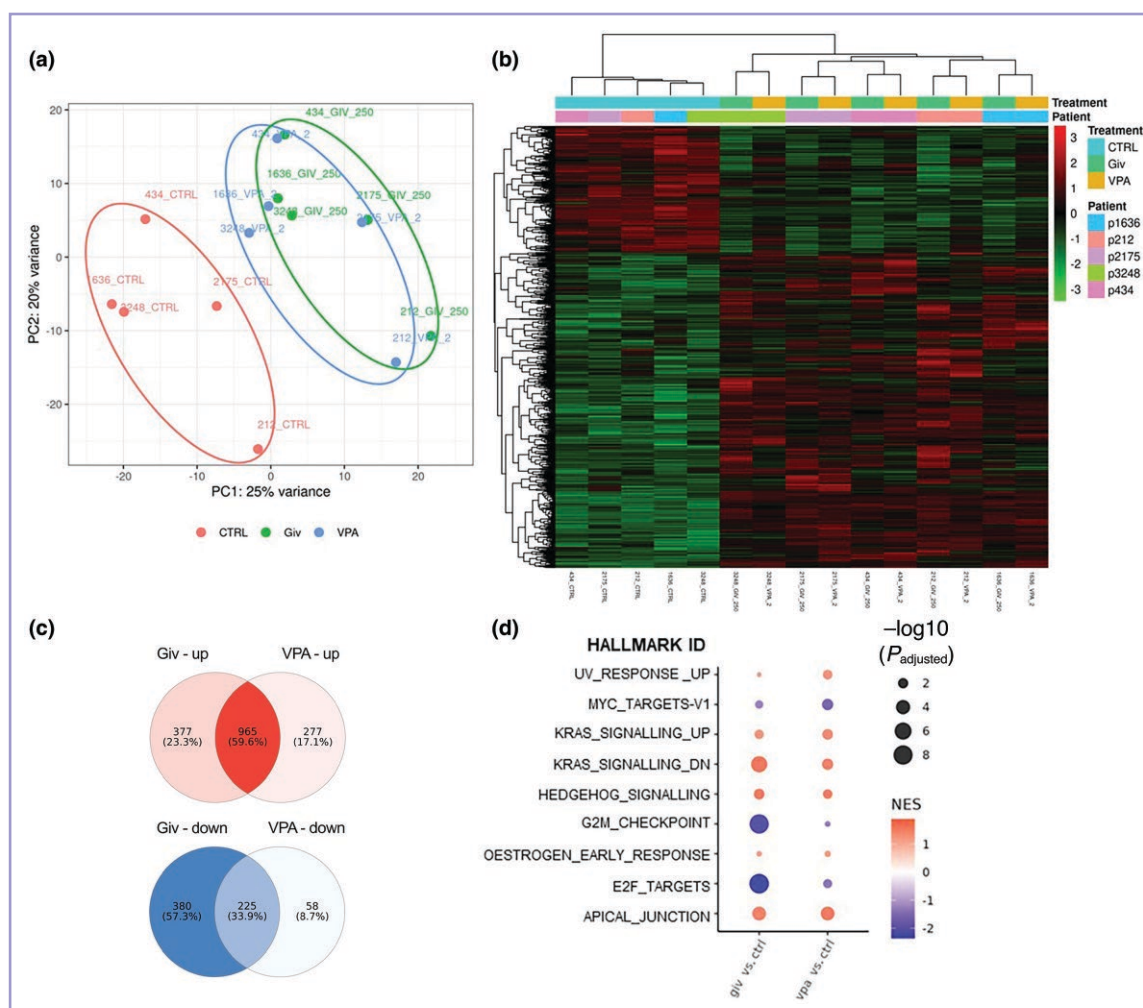
Enrichment analysis based on hallmark gene set collection indicated that mRNA for genes involved in apical junction and Sonic Hedgehog pathways was upregulated, while mRNA for genes responsible for cell cycle progression (G_2–M transition, E2F targets, Myc targets) was downregulated (Figure 3d). In addition, the expression levels of genes involved in k-Ras signalling up- and down-regulation were increased. Analysis carried out on KEGG (Kyoto Encyclopedia of Genes and Genomes) pathways confirmed some results (enrichment of cell junction and cell adhesion molecules; Sonic Hedgehog signalling) (Figure S4; see Supporting Information).

Real-time quantitative polymerase chain reaction (qPCR) validation of a set of differentially expressed genes was performed on RNA samples obtained after a second round of treatment, and from the fibroblasts of an additional three patients ($n = 8$; Figure 4a). The expression levels of genes related to cell proliferation (*PCNA*, *AURKA*, *TP53*, *CDK1* and *CDK3*) decreased significantly in givinostat-treated fibroblasts compared with vehicle-treated fibroblasts; this was also true for *AURKA*, *TP53* and *CDK3* in VPA-treated cells.

Figure 2 Givinostat and valproic acid treatment exerts antifibrotic properties on recessive dystrophic epidermolysis bullosa (RDEB) fibroblasts. (a) Representative image of collagen lattice contraction assays 48 h after gel detachment from the well. Dotted red circles indicate collagen gel edges. Fibroblasts were treated with vehicle (CTRL), 250 nmol L⁻¹ givinostat (Giv) or 2 mmol L⁻¹ VPA for 72 h. The cells were then washed, detached, counted and seeded into wells with collagen. After collagen polymerization, the gels were detached from the wells to allow contraction and their area analysed at 8 h, 24 h and 48 h. (Bottom) Histogram with individual values of gel areas at 48 h, expressed as percentage of areas at gel detachment. (b, top) Western blot for α-smooth muscle actin (SMA) showing reduced intensity of the specific signal in proteins extracted from collagen gels seeded with RDEB fibroblasts pretreated with histone deacetylase inhibitors (HDACi). Vinculin was analysed as a loading control. (Bottom) Histogram showing individual values of α-SMA/vinculin band intensity. (c, left) Representative immunofluorescence images for α-SMA (red staining) in RDEB fibroblasts treated or not (CTRL) with HDACi for 72 h. (c, right) Histogram showing fluorescence staining intensity for α-SMA in RDEB fibroblasts treated with vehicle (CTRL), 250 nmol L⁻¹ givinostat or 2 mmol L⁻¹ VPA for 72 h. Nuclei are stained with 4′,6-diamidino-2-phenylindole (DAPI; blue). Scale bars = 20 μm. (d) Transforming growth factor (TGF)-β1 levels in the supernatants of collagen gels seeded with RDEB fibroblasts pretreated with HDACi or not (CTRL). Owing to the high variability of TGF-β1 released under the basal condition, values are expressed as a percentage of the concentrations obtained in vehicle-treated cells (CTRL), which are considered as 100%. (e) Levels of cytokines/chemokines released in collagen lattice supernatants. Values are normalized to those of CTRL, expressed as 100%. IL, interleukin; MCP, monocyte chemoattractant protein; VEGF, vascular endothelial growth factor. *$P < 0.05$; **$P < 0.01$; ***$P < 0.005$.

Figure 3 Transcriptional effects of pan-histone deacetylase inhibitor (HDACi) administration to recessive dystrophic epidermolysis bullosa (RDEB) fibroblasts. (a) Principal component (PC) analysis plot showing the similarity of samples analysed, after data processing and normalization. HDACi-treated samples tend to cluster away from vehicle-treated controls (CTRL). (b) Heatmap with normalized expression of transcripts that were similarly regulated in RDEB fibroblasts after 30 h of givinostat (Giv) or valproic acid (VPA) treatment (red = upregulated; green = downregulated). (c) Total number of genes regulated after HDACi treatment in RDEB fibroblasts. The number and percentage of genes commonly upregulated ('up'; red) or downregulated ('down'; blue) after treatment with givinostat and VPA are shown in the intersections. (d) Gene set enrichment analysis based on the hallmark gene set collection in both VPA- and givinostat-treated cells (red = positively enriched; blue = negatively enriched). The highest-ranked gene sets are shown according to the adjusted *P*-value (–log10). NES, normalized enrichment score.

Therefore, cell proliferation was analysed in RDEB fibroblasts treated with 250 nmol L^{-1} givinostat or 2 mmol L^{-1} VPA for 24 h, 48 h and 72 h (Figure 4b). At 72 h, the percentage of proliferating cells treated with givinostat or VPA was significantly lower than in vehicle-treated cells.
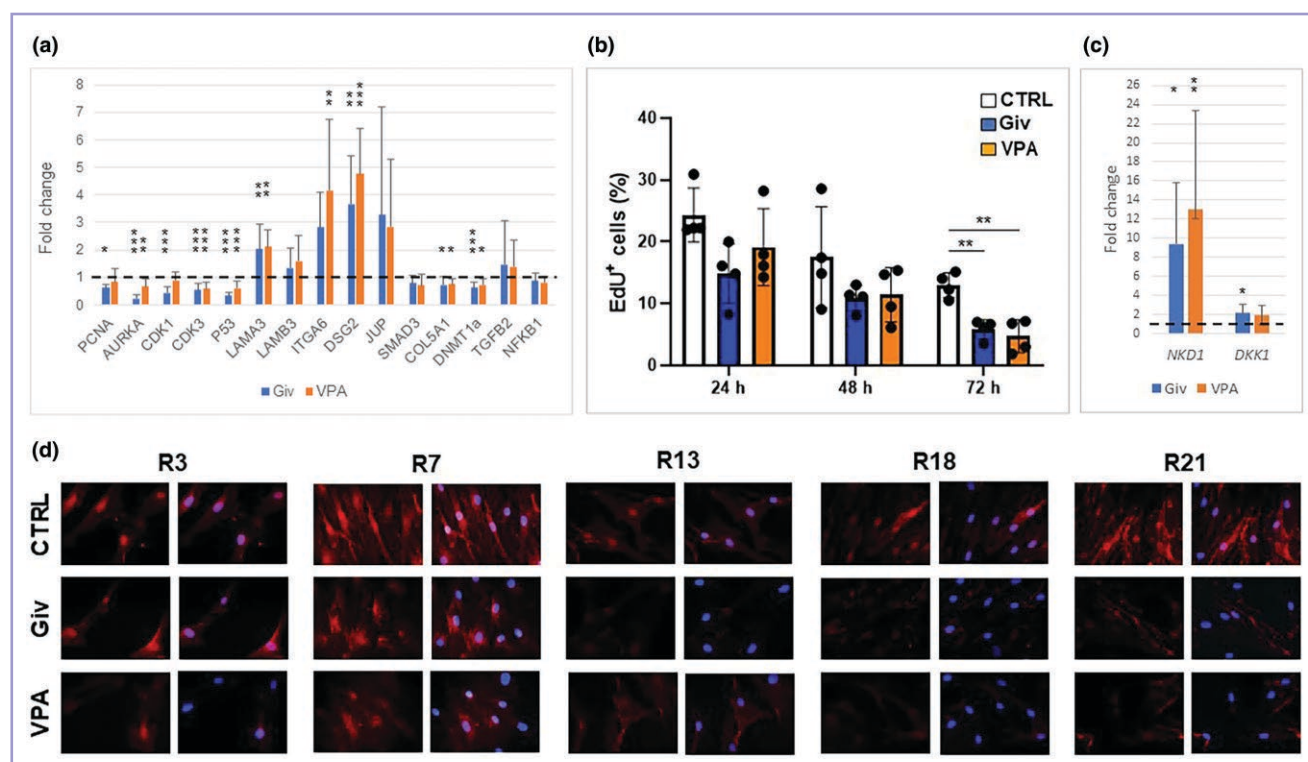
As for adhesion molecules, genes encoding the α3 and β3 subunits of laminin 332 (*LAMA3* and *LAMB3*) and integrin-α6 (*ITGA6*), and for two desmosome components, desmoglein-2 (*DSG2*) and plakoglobin (*JUP*), were evaluated. All were expressed at higher levels in HDACi-treated cells vs. untreated ones; significant differences were found for *LAMA3*, *ITGA6* and *DSG2* (Figure 4a). Genes with crucial activities in Sonic Hedgehog signalling (*PTCH*, *DSH* and *GLI1*) showed undetectable expression levels in both basal conditions and after HDACi treatment (data not shown).

Among the genes that did not emerge from enrichment analysis, *SMAD3* and *TGFB2*, which have a role in TGF-β signalling, and *COL5A1* and *NFKBI*, which mediate fibrotic

processes, were differentially expressed by RNA-Seq, but only *COL5A1* was confirmed by real-time qPCR as being significantly decreased (Figure 4a). Downregulation of *DNMT1*, which encodes DNA methyltransferase 1 (DNMT1; responsible for the maintenance of DNA methylation), was confirmed in cells treated with both HDACi (Figure 4a). Moreover, the Wnt inhibitors *NKD1* and *DKK1* were significantly upregulated (Figure 4c). Analysis of canonical Wnt signalling activation, investigated by detecting β-catenin nuclear localization, showed a tendency of nuclear localization to be lost in RDEB fibroblasts following HDACi administration for 72 h (Figure 4d).

Valproic acid counteracts the development of secondary disease manifestations in recessive dystrophic epidermolysis bullosa mice

To evaluate the therapeutic potential of HDACi treatment in RDEB, givinostat and VPA were administered to mice

Figure 4 Validation of RNA sequencing (RNA-Seq) data. (a) Real-time quantitative polymerase chain reaction (qPCR) analysis to validate differentially expressed genes identified by RNA-Seq on mRNA from recessive dystrophic epidermolysis bullosa (RDEB) fibroblasts (*n*=8) treated with vehicle, givinostat (Giv) 250 nmol L⁻¹ or valproic acid (VPA) 2 mmol L⁻¹ for 30 h. Values are normalized to those of vehicle-treated cells (dotted bar). (b) Proliferation analysis of RDEB fibroblasts treated with histone deacetylase inhibitors (HDACi) for 24 h, 48 h or 72 h, expressed as percentage of proliferating cells. (c) Real time qPCR analysis of the Wnt inhibitors *NKD1* and *DKK1* on mRNA from RDEB fibroblasts (*n*=8) treated for 30 h with vehicle, givinostat 250 nmol L⁻¹ or VPA 2 mmol L⁻¹. Values are normalized to those of vehicle-treated cells (dotted bar). (d) Immunofluorescence for β-catenin on fibroblasts from people with RDEB (R) treated with vehicle (CTRL), givinostat 250 nmol L⁻¹ or VPA 2 mmol L⁻¹ for 72 h. Loss of nuclear staining was detected after HDACi treatment, although not uniformly in all patients. Images on the right were obtained by merging β-catenin staining with nuclear staining [4′,6-diamidino-2-phenylindole (DAPI)]. *P<0.05; **P<0.01; ***P<0.005.

expressing residual levels of C7 (*Col7a1^flNeo/flNeo* mice), a pre-clinical model of RDEB (henceforth referred to as 'RDEB mice').[26,28] Immunofluorescence staining for Ac-H3 was significantly reduced in the skin of 14-week-old RDEB mice compared with wild-type (WT) mice (Figure S5a; see Supporting Information).[17] Western blot analysis of skin protein extracts confirmed this reduction (Figure S5b).

HDACi were administered to the animals' food, starting at the weaning stage, for 13 weeks (Figure S5c). Water and dimethyl sulfoxide (DMSO) were used as control treatments for VPA and givinostat, respectively. WT littermates were included as a reference group.

A dosage of 30 mg kg⁻¹ daily was chosen for givinostat because it is close to the maximum dose given systemically to mice over a long period.[29] No clear phenotypic difference was observed between the treated mice and RDEB controls at the endpoint (data not shown). Accordingly, Ac-H3 levels were not found to be increased in the skin of givinostat-treated mice vs. RDEB controls by Western blot (Figure S5d). This finding suggests that delivery of givinostat to the skin was ineffective. The effect of givinostat administration was not further analysed.

With regard to VPA, a dosage of 1.5 g kg⁻¹ daily was tested.[30] VPA- and vehicle-treated RDEB mice were comparable in mean weight and forepaw condition at the start
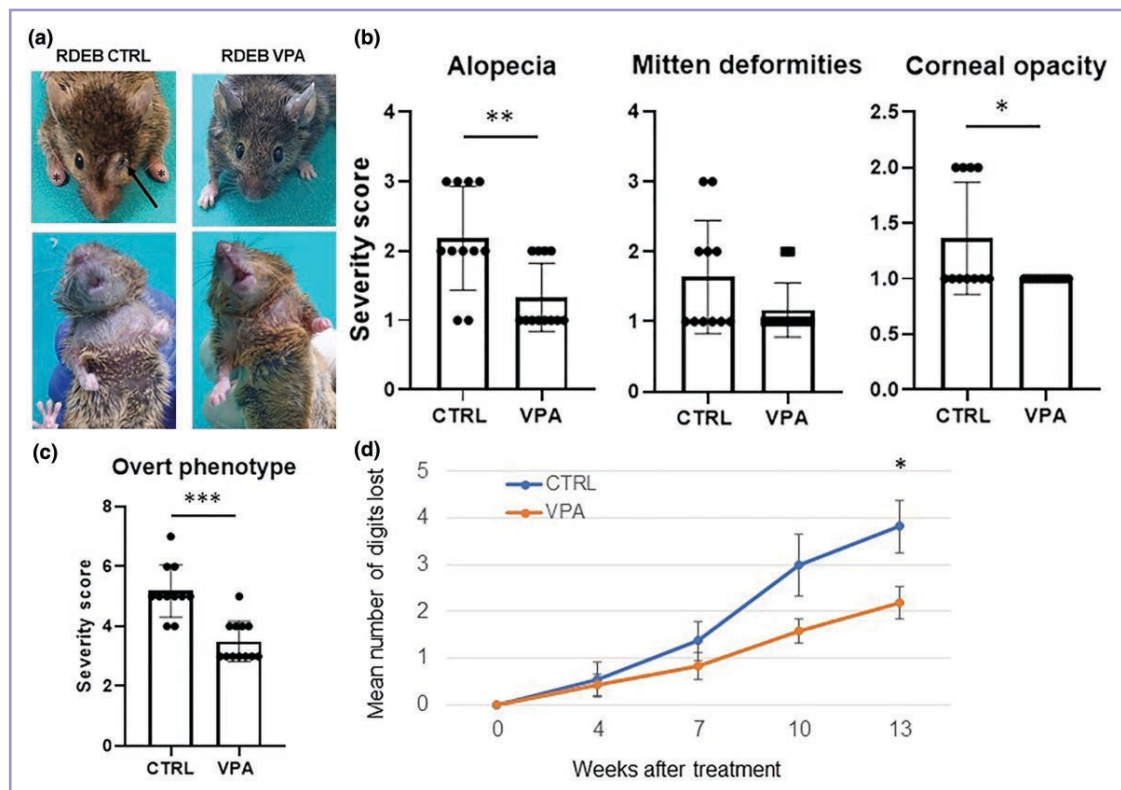
of treatment (Table S3; see Supporting Information). Sixteen RDEB mice in each experimental group were treated; of these, nine were euthanized before the endpoint (vehicle group, *n*=5; VPA group, *n*=4), owing to considerable weight loss and/or poor health condition.

At the endpoint, VPA levels were monitored in the blood 4 h or 24 h after drug administration (Figure S5e); mean levels were 75 (43) μg mL⁻¹ at 4 h (in humans, effective and nontoxic levels are between 50 and 100 μg mL⁻¹). Histone acetylation levels in the skin, assessed by Western blot and immunohistochemistry, were significantly increased in VPA-treated samples compared with vehicle-treated samples (Figure S5f).

Mice treated with VPA showed improved general condition at the study endpoint (Figure 5a). A gravity score was given, considering three parameters: alopecia extension, corneal opacity and mitten deformities (Table S4; see Supporting Information). All scores were lower in VPA-treated mice than in those treated with vehicle (Figure 5b, c).

Digit contraction and digit loss were evaluated at 0, 4, 7, 10 and 13 weeks of treatment. No significant differences were found in digit length (data not shown). Mean digit loss was reduced in VPA-treated mice starting from 7 weeks and was significantly lower compared with control RDEB mice at 13 weeks [2.3 (1.9) vs. 3.8 (1.9); *P*<0.05] (Figure 5d).

Figure 5 Improved overt phenotype of recessive dystrophic epidermolysis bullosa (RDEB) mice treated with valproic acid (VPA). (a) Representative images of RDEB mice treated with vehicle (CTRL) or VPA. Control RDEB mice showed a worse overall overt phenotype with wider areas of alopecia, increased presence of eye abnormalities (corneal opacity, arrow) and increased development of mitten deformities in the forepaws (asterisks). (b) Gravity score for three parameters: presence and extent of alopecia; corneal opacity; and development of mitten deformities. Score values [from 1 (best condition) to 3 (worst condition)] for each parameter are provided in Table S4. The scores were higher for the three parameters and significantly different for alopecia and corneal opacity in vehicle-treated mice compared with VPA-treated mice. Statistical analysis was performed using a two-tailed Student's *t*-test after testing for normality of sample distribution using the D'Agostino–Pearson test. (c) Global severity score (overt phenotype) with the sum of the values for the three parameters evaluated. (d) Digit loss, expressed as mean number of digits lost, in vehicle-treated (CTRL) and VPA-treated RDEB mice. The number of digits lost was progressively higher in vehicle-treated mice vs. VPA-treated mice and was significantly different after 13 weeks of treatment. $*P < 0.05$; $**P < 0.01$; $***P < 0.005$.

Valproic acid counteracts skin fibrosis in recessive dystrophic epidermolysis bullosa mice

The effect of VPA administration was analysed in dorsal skin; this area is much less exposed to mechanical stress than the forepaws, so fibrosis might be expected to result mainly from microenvironmental changes elicited by inadequate C7 rather than from repeated blistering. Strongly reduced hypodermal fat tissue – a trait of fibrotic skin[31–33] – was found in samples of vehicle-treated mice, while fat tissue thickness was similar in VPA-treated and WT skin (Figure 6a). Dermal thickness was comparable among the three experimental groups.

The analysis of picrosirius red-stained skin sections showed a decrease in the ratio of large or parallel red/orange collagen bundles to thin or random green bundles in VPA-treated mice (Figure 6b). These data indicate that collagen bundle organization is relaxed following VPA treatment. Masson's trichrome staining, which highlights the amount of collagen fibres, was similar between vehicle-treated and VPA-treated mice (not shown).
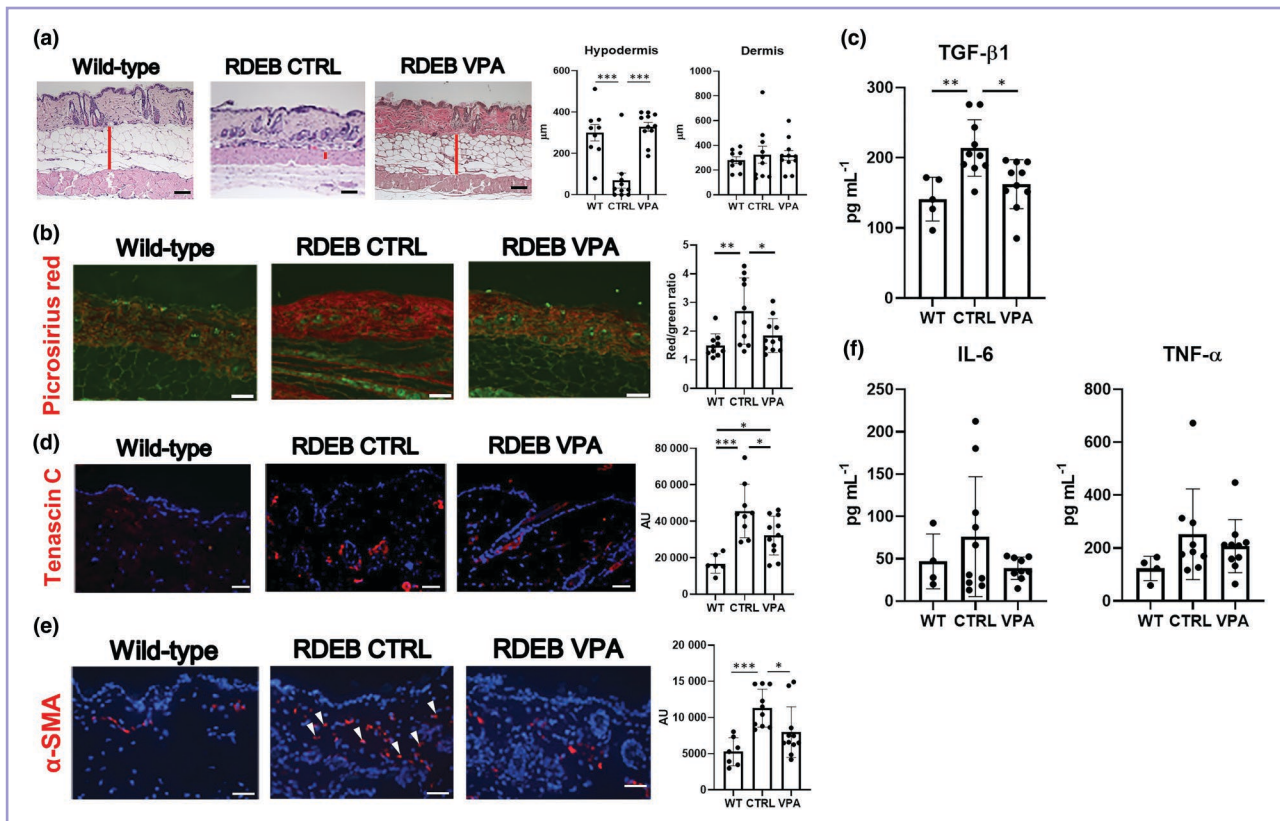
ELISA of proteins extracted from full-thickness dorsal skin samples showed decreased levels of TGF-β1 in VPA-treated mice (Figure 6c). Immunofluorescence for two markers of fibrosis – the glycoprotein tenascin C (expressed during wound healing and in pathological conditions)[34] and α-SMA – showed decreased levels in the dermis of VPA-treated mice vs. those treated with vehicle (Figure 6d, e). ELISA of protein skin extracts did not reveal a significant difference in the levels of the inflammatory cytokines IL-6 and TNF-α among the experimental groups (Figure 6f).

Having found that cell proliferation was decreased following VPA treatment *in vitro*, skin sections from RDEB mice were analysed by immunohistochemistry for the proliferation marker Ki67. A similar mean percentage of stained nuclei was found in interfollicular basal keratinocytes [WT 9.1% (3.6); RDEB control 8.8% (4.1); RDEB treated with VPA 8.6% (3.3)], while rare isolated positive cells were found within the dermis of mice from the three experimental groups (data not shown).

To investigate whether systemic defects were counteracted by VPA treatment, histological sections from the tongues and eyes of mice were analysed. For tongue tissue, the presence of epithelial filiform papillae, epithelial hyperplasia and large blisters was evaluated (Figure S6a, b; see Supporting Information).[35,36] In RDEB control mice,

Figure 6 Valproic acid (VPA) treatment counteracts fibrosis progression in the skin of recessive dystrophic epidermolysis bullosa (RDEB) mice. (a) Representative images of haematoxylin and eosin-stained dorsal skin showing a strong reduction in fat tissue (red bars) in vehicle-treated RDEB mice. VPA-treated mice showed adipose tissue similar to wild-type (WT) mice (right). Analysis of dermal thickness showed similar values in the three experimental groups. Scale bars = 100 μm. Data are expressed as mean (SEM). (b) Picrosirius red staining of dorsal skin specimens analysed under a polarized filter. Parallel or large fibrillar collagen bundles are stained in red/orange. Stronger red/orange staining is seen in the skin of vehicle-treated RDEB mice (CTRL) vs. both WT mice and VPA-treated RDEB mice. The histogram (right) shows the differences in the three experimental groups, with values expressed as red/green ratio (green stains random or thin collagen bundles). Scale bars = 100 μm. (c) Enzyme-linked immunosorbent assay (ELISA) for transforming growth factor (TGF)-β1 in proteins extracted form dorsal skin, expressed as pg mL^{-1}. (d) Immunofluorescence for the fibrosis-associated protein tenascin C in the skin. The histogram with individual values (right) shows that the signal was significantly increased in the skin of vehicle-treated RDEB mice (CTRL) compared with both WT mice and VPA-treated RDEB mice. Scale bars = 50 μm. (e) Immunofluorescence for α-smooth muscle actin (SMA) on the dorsal skin of WT, vehicle-treated and VPA-treated mice, and histogram with individual values (right). α-SMA also stains pericytes surrounding arterioles and is therefore normally detected in the dermis; staining of individual cells was increased in the dermis of vehicle-treated RDEB mice (arrowheads), while fluorescence intensity was similar in WT mice and VPA-treated mice. Scale bars = 50 μm. (f) ELISA for interleukin (IL)-6 and tumour necrosis factor (TNF)-α in skin protein extracts. AU, arbitrary units. *$P < 0.05$; **$P < 0.01$; ***$P < 0.005$.

extensive blisters, diffused epithelial hyperplasia and loss of filiform papillae were found. The same defects were present in a lower percentage of VPA-treated mice. With regard to eyes, corneal tissue was analysed by evaluating epithelial hyperplasia, blisters and ulcerations (Figure S6d, e).[28] Epithelial hyperplasia and ulcerations were more frequently found in vehicle-treated RDEB mice than in those treated with VPA. Immunofluorescence for TGF-β revealed reduced staining intensity in the tongue and eye tissue of VPA-treated mice vs. those treated with vehicle (Figure S6c, f; see Supporting Information).

Valproic acid administration normalizes expression of genes involved in protein synthesis and immune function in the skin of recessive dystrophic epidermolysis bullosa mice

To delineate the molecular effects of VPA underlying the attenuation of skin fibrosis in RDEB mice, mass spectrometry-based proteomic analysis was performed on proteins extracted from dorsal skin ($n = 3$). Hierarchical clustering of protein abundance revealed changes that were grouped into five clusters (Figure S7a; see Supporting Information). Clusters 1 and 3 included those for which protein levels differed between VPA- and vehicle-treated RDEB mice, whereas they were similar between VPA-treated and WT mice (Figure S7b, d). Pathway enrichment analyses indicated that downregulated proteins in cluster 1 were associated with ribosomal proteins/translation, while upregulated proteins in cluster 3 were associated with immune response and endosome/endocytosis/lysosomes. For clusters 4 (glycolysis) and 5 (endoplasmic reticulum, protein transport, protease inhibitor activity), VPA-treated skin showed decreased expression levels vs. both WT and vehicle-treated RDEB mice. In contrast to glycolysis, lipid metabolism and mitochondrial activity were increased in RDEB mice vs. WT mice and were not affected following VPA treatment (cluster 2).

Discussion

RDEB can be highly disabling – the most severe forms can result in early mortality. There is no curative treatment. Marked phenotypic variability has been described in siblings with RDEB, including in monozygotic twins,[7,24,25] suggesting that epigenetic modifiers may be involved in disease progression. In this study, we found that reduced histone protein acetylation is present in RDEB skin and cultured fibroblasts.

Histone deacetylation has been linked to tissue fibrosis in different pathologies, where the inhibition of HDACs proved effective in reverting fibrosis.[37] Pan-HDACi administration was also found to counteract fibrosis in both *in vitro* and *in vivo* skin models of hypertrophic scarring, keloids and systemic scleroderma.[38–41]

We tested the effect of HDACi administration on RDEB fibroblasts that manifested profibrotic behaviour.[6,7] Two pan-HDACi – givinostat and VPA – were able to counteract RDEB fibroblast contractility, reducing α-SMA expression and TGF-β1 release. The effect of HDACi was then tested in RDEB mice.[26] Following long-term systemic treatment with VPA, RDEB mice manifested a better disease phenotype than those treated with vehicle. Accordingly, skin fibrosis was counteracted. These effects were associated with decreased TGF-β levels. These data indicate that histone deacetylation sustains TGF-β-dependent progressive fibrosis in RDEB and that the systemic administration of pan-HDACi counteracts the development of disabling disease complications.

Transcriptomic analysis in RDEB fibroblasts and proteomic analysis in VPA-treated mouse skin revealed partly overlapping aspects of HDACi activity. With regard to transcriptomics, the main effect of HDACi administration was a reduction in the expression of genes involved in cell proliferation. Consistent with these findings, a decrease in RDEB fibroblast proliferation was observed following HDACi administration. This reduction in cell proliferation is a known effect exerted by VPA;[42] however, when the skin of VPA-treated mice was analysed for Ki67 expression by immunohistochemistry no difference in positive cells was found in the three experimental groups, both in basal keratinocytes and in the dermis, where only occasional stained nuclei were detected. This finding is not surprising if one considers that – as opposed to cultured fibroblasts – unwounded skin is in a quiescent status and RDEB mice do not spontaneously develop epidermal tumours.[26]

Two inhibitors of Wnt – an activator of fibrosis[19] – were upregulated at the mRNA level after HDACi treatment. This finding correlates with a reduction in nuclear β-catenin. An increase in the Wnt inhibitor secreted frizzled-related protein 1 (SFRP1) was reported in keloid fibroblasts treated with the pan-HDACi trichostatin,[43] suggesting that pan-HDACi may exert antifibrotic activity by inhibiting this pathway. With regard to RDEB, Wnt5a ligand expression is increased in RDEB dermal matrix and cultured fibroblasts following *COL7A1* knockdown.[44] TGF-β was shown to repress the expression of the Wnt inhibitors Dickkopf-related protein 1 (DKK1) and SFRP1 by inducing DNA methyltransferase expression which, in turn, promotes gene promoter hypermethylation.[45] As we found a decrease in *DNMT1* levels following HDACi administration, it can be hypothesized that the interplay of TGF-β, DNMT1 and Wnt sustains the profibrotic activity of RDEB fibroblasts, while HDACi administration counteracts it.

Proteomic analysis of mouse skin revealed interesting aspects of VPA activity that deserved further evaluation. The reduction in ribosome proteins – also observed by RNA-Seq in VPA-treated RDEB fibroblasts – highlights a decrease in protein synthesis following VPA treatment. In this regard, the pathway of ribosome biogenesis was found to be among the most upregulated in human postradiotherapy fibrotic skin.[46] Moreover, enhanced protein synthesis is a feature of activated protumorigenic cells.[47] VPA is being tested in cancer treatment at the clinical level, as a co-adjuvant in chemotherapy.[48,49] Decreasing cell activation may have a role not only in counteracting the development of a fibrotic environment, but also in halting a protumorigenic cell behaviour.

HDAC activity is modulated during skin repair and class I and II HDACi administration accelerates healing in acute and delayed wound models by improving the activity of different cell populations at the wound site.[50] Skin repair is delayed in RDEB mice;[3] therefore, it may be hypothesized that VPA treatment also improves the healing of skin and mucosal lesions. However, it was shown that molecular responses to skin injury promote a kind of epigenetic memory in epithelial stem cells, even in those distant from the site of injury, making them ready to respond efficiently to subsequent wounds.[51] These changes may also promote tumorigenesis. Inhibiting wound-induced epigenetic changes may protect skin from local and distant cell overactivation and tumorigenesis.

Proteins involved in immune response [major histocompatibility complex (MHC) protein complex], endosomes, endocytosis and lysosomes clustered and were upregulated in VPA-treated vs. vehicle-treated RDEB mice. Like people with RDEB, mice with RDEB manifest increased bacterial skin colonization in lesional and nonlesional skin.[52] This defect is caused by the loss of C7 from secondary lymphoid organs, resulting in an inability to sustain a proper innate immune response against bacterial challenges.[52] It has long been known that endosomal/lysosomal proteolysis generates peptides that bind MHC molecules in antigen processing and presentation, a process of fundamental importance to immunity to pathogens.[53] These proteomic findings point to a potential effect of VPA in reinforcing an impaired immune response in RDEB.

Proteomic analysis of mouse skin also indicated that VPA administration correlated with decreased expression levels of proteins involved in glycolysis. Glycolytic metabolism has been associated with fibroblast activation in other fibrotic skin disorders, such as systemic sclerosis and keloids,[54–56] and the use of compounds inhibiting glycolysis has been suggested for the treatment of skin fibrosis.[54] Moreover, these data are in line with the ability of VPA to counteract the progression of TGF-β-induced fibrosis, as TGF-β enhances glycolysis and lactic acid production, which – in turn – promotes myofibroblast differentiation.[57]

Major ECM components, primarily fibrillar collagens, were not changed significantly in the skin of VPA-treated mice, as assessed with proteomics, Masson's trichrome staining and dermal thickness analysis. These findings support the concept that abnormal matrix organization, rather than

increased levels of matrix protein, is associated with skin fibrosis in RDEB.[27]

Inflammation is considered central for the onset and progression of fibrosis. Release of a subset of cytokines/chemokines was increased in HDACi-treated RDEB fibroblasts. The *in vivo* analysis revealed that IL-6 and TNF-α did not decrease in the skin of VPA-treated vs. vehicle-treated skin. These findings are reminiscent of data obtained on decorin administration to RDEB mice where antifibrotic effects were not associated with reduced inflammation.[17] It has been shown that C7 deficiency changes the proteome, which may alter TGF-β bioavailability in the absence of increased skin inflammation;[9] thus, the onset and progression of fibrosis are likely to depend closely on increased TGF-β rather than on inflammation in an RDEB pathological context.

To conclude, we have shown that histone acetylation is altered in the progressive fibrosis paradigmatic skin disorder RDEB. We also found that the pan-HDACi VPA – by rescuing histone acetylation levels – mitigates fibrosis-mediated disease complications in an RDEB model. Systemic administration of HDACi may therefore be considered for counteracting fibrosis in symptomatic treatments for RDEB.

Conflicts of interest

The authors declare no conflicts of interest.

Data availability

RNA sequencing data were deposited in Gene Expression Omnibus (GEO) under accession number GSE239569. The mass spectrometry proteomics data were deposited in the ProteomeXchange Consortium via the PRIDE partner repository with the dataset identifier PXD047998. The data underlying this article will be shared upon reasonable request to the corresponding author.

Ethics statement

Studies on human cells were approved by the Committee on Human Experimentation of IDI-IRCCS (protocol no. 578). Patients and healthy donors gave informed written consent. The study was conducted according to the principles of the Declaration of Helsinki. Animal experimentation was approved by the animal welfare arm of IDI-IRCCS and authorized by the Animal Committee of the Italian Ministry of Health (protocol no. BBA76.4, approval no. 72/2019-PR).

Supporting Information

Additional Supporting Information may be found in the online version of this article at the publisher's website.

References

1 Bardhan A, Bruckner-Tuderman L, Chapple ILC *et al.* Epidermolysis bullosa. *Nat Rev Dis Primers* 2020; **6**:78.

2 Nyström A, Bruckner-Tuderman L, Kiritsi D. Dystrophic epidermolysis bullosa: secondary disease mechanisms and disease modifiers. *Front Genet* 2021; **12**:737272.

3 Nyström A, Velati D, Mittapalli VR *et al.* Collagen VII plays a dual role in wound healing. *J Clin Invest* 2013; **123**:3498–509.

4 Cianfarani F, Zambruno G, Castiglia D, Odorisio T. Pathomechanisms of altered wound healing in recessive dystrophic epidermolysis bullosa. *Am J Pathol* 2017; **187**:1445–53.

5 Guerra L, Odorisio T, Zambruno G, Castiglia D. Stromal microenvironment in type VII collagen-deficient skin: the ground for squamous cell carcinoma development. *Matrix Biol* 2017; **63**:1–10.

6 Küttner V, Mack C, Rigbolt KTG *et al.* Global remodelling of cellular microenvironment due to loss of collagen VII. *Mol Syst Biol* 2013; **9**:657.

7 Odorisio T, Di Salvio M, Orecchia A *et al.* Monozygotic twins discordant for recessive dystrophic epidermolysis bullosa phenotype highlight the role of TGF-β signalling in modifying disease severity. *Hum Mol Genet* 2014; **23**:3907–22.

8 Cao Q, Tartaglia G, Alexander M *et al.* Collagen VII maintains proteostasis in dermal fibroblasts by scaffolding TANGO1 cargo. *Matrix Biol* 2022; **111**:226–44.

9 Atenasova VS, Russell RJ, Webster TG *et al.* Thrombospondin-1 is a major activator of TGF-β signaling in recessive dystrophic epidermolysis bullosa fibroblasts. *J Invest Dermatol* 2019; **139**:1497–505.

10 Darby IA, Zakuan N, Billet F, Desmoulière A. The myofibroblast, a key cell in normal and pathological tissue repair. *Cell Mol Life Sci* 2016; **73**:1145–57.

11 Desmouliere A, Redard M, Darby I, Gabbiani G. Apoptosis mediates the decrease in cellularity during the transition between granulation tissue and scar. *Am J Pathol* 1995; **146**:56–66.

12 Subramaniam KS, Antoniou MN, McGrath JA, Lwin SM. The potential of gene therapy for recessive dystrophic epidermolysis bullosa. *Br J Dermatol* 2022; **186**:609–19.

13 Hou PC, Del Agua N, Lwin SM *et al.* Innovations in the treatment of dystrophic epidermolysis bullosa (DEB): current landscape and prospects. *Therap Clin Risk Manag* 2023; **19**:455–73.

14 Gurevich I, Agarwal P, Zhang PP *et al.* In vivo topical gene therapy for recessive dystrophic epidermolysis bullosa: a phase 1 and 2 trial. *Nat Med* 2022; **28**:780–8.

15 Guide VS, Gonzalez ME, I Sinem Bağcıet IS *et al.* Trial of Beremagene Geperpavec (B-VEC) for dystrophic epidermolysis bullosa. *N Engl J Med* 2022; **387**:2211–19.

16 Nyström A, Thriene K, Mittapalli V *et al.* Losartan ameliorates dystrophic epidermolysis bullosa and uncovers new disease mechanisms. *EMBO Mol Med* 2015; **7**:1211–28.

17 Cianfarani F, De Domenico E, Nyström A *et al.* Decorin counteracts disease progression in mice with recessive dystrophic epidermolysis bullosa. *Matrix Biol* 2019; **81**:3–16.

18 Liu Y, Wen D, Ho C *et al.* Epigenetics as a versatile regulator of fibrosis. *J Transl Med* 2023; **21**:164.

19 Dees C, Chakraborty D, Distler JHW. Cellular and molecular mechanisms in fibrosis. *Exp Dermatol* 2021; **30**:121–31.

20 Park SY, Kim JS. A short guide to histone deacetylases including recent progress on class II enzymes. *Exp Mol Med* 2020; **52**:204–12.

21 Pang M, Zhuang S. Histone deacetylase: a potential therapeutic target for fibrotic disorders. *J Pharmacol Exp Ther* 2010; **335**:266–72.

22 Jones DL, Haak AJ, Caporarello NC *et al.* TGFβ-induced fibroblast activation requires persistent and targeted HDAC-mediated gene repression. *J Cell Sci* 2019; **18**:132.

23 Bodemer C, Igondjo Tchen S, Ghomrasseni S *et al.* Skin expression of metalloproteinases and tissue inhibitor of metalloproteinases in sibling patients with recessive dystrophic epidermolysis and intrafamilial phenotypic variation. *J Invest Dermatol* 2003; **121**:273–9.

24 Titeux M, Pendaries V, Tonasso L *et al.* A frequent functional SNP in the MMP1 promoter is associated with higher disease severity in recessive dystrophic epidermolysis bullosa. *Hum Mutat* 2008; **29**:267–76.

25 Chacón-Solano E, León C, Carretero M *et al.* Mechanistic interrogation of mutation-independent disease modulators of RDEB identifies the small leucine-rich proteoglycan PRELP as a TGF-β antagonist and inhibitor of fibrosis. *Matrix Biol* 2022; **111**:189–206.

26 Fritsch A, Loeckermann S, Kern JS *et al.* A hypomorphic mouse model of dystrophic epidermolysis bullosa reveals mechanisms of disease and response to fibroblast therapy. *J Clin Invest* 2008; **118**:1669–79.

27 Bernasconi R, Thriene K, Romero-Fernández E *et al.* Pro-inflammatory immunity supports fibrosis advancement in epidermolysis bullosa: intervention with Ang-(1-7). *EMBO Mol Med* 2021; **13**:e14392.

28 Chen VM, Shelke R, Nyström A *et al.* Collagen VII deficient mice show morphologic and histologic corneal changes that phenotypically mimic human dystrophic epidermolysis bullosa of the eye. *Exp Eye Res* 2018; **175**:133–41.

29 Licandro SA, Crippa L, Pomarico R *et al.* The pan HDAC inhibitor Givinostat improves muscle function and histological parameters in two Duchenne muscular dystrophy murine models expressing different haplotypes of the LTBP4 gene. *Skelet Muscle* 2021; **11**:19.

30 Scholz B, Schulte JS, Hamer S *et al.* HDAC (Histone Deacetylase) inhibitor valproic acid attenuates atrial remodeling and delays the onset of atrial fibrillation in mice. *Circ Arrhythm Electrophysiol* 2019; **12**:e007071.

31 Fleischmajer R, Damiano V, Nedwich A. Scleroderma and the subcutaneous tissue. *Science* 1971; **171**:1019–21.

32 Sonnylal S, Denton CP, Zheng B *et al.* Postnatal induction of transforming growth factor beta signaling in fibroblasts of mice recapitulates clinical, histologic, and biochemical features of scleroderma. *Arthritis Rheum* 2007; **56**:334–44.

33 Goncalves Marangoni R, Korman BD, Wei J *et al.* Myofibroblasts in murine cutaneous fibrosis originate from adiponectin-positive intradermal progenitors. *Arthritis Rheumatol* 2015; **67**:1062–73.

34 Bhattacharyya S, Wang W, Morales-Nebreda L *et al.* Tenascin-C drives persistence of organ fibrosis. *Nat Commun* 2016; **7**:11703.

35 Wright JT. Oral manifestations in the epidermolysis bullosa spectrum. *Dermatol Clin* 2010; **28**:159–64.

36 Krämer S, Fuentes I, Yubero MJ *et al.* Absence of tongue papillae as a clinical criterion for the diagnosis of generalized recessive dystrophic epidermolysis bullosa types. *J Am Acad Dermatol* 2020; **83**:1815–16.

37 Yoon S, Kang G, Hyeon Eom G. HDAC inhibitors: therapeutic potential in fibrosis-associated human diseases. *Int J Mol Sci* 2019; **20**:1329.

38 Diao JS, Xia WS, Yi CG *et al.* Trichostatin A inhibits collagen synthesis and induces apoptosis in keloid fibroblasts. *Arch Dermatol Res* 2011; **303**:573–80.

39 Tu T, Huang J, Lin M *et al.* CUDC–907 reverses pathological phenotype of keloid fibroblasts in vitro and in vivo via dual inhibition of PI3 K/Akt/mTOR signaling and HDAC2. *Int J Mol Med* 2019; **44**:1789–800.

40 Henderson J, Distler J, O'Reilly S. The role of epigenetic modifications in systemic sclerosis: a druggable target. *Trends Mol Med* 2019; **25**:395–411.

41 Diao JS, Xia WS, Yi CG *et al.* Histone deacetylase inhibitor reduces hypertrophic scarring in a rabbit ear model. *Plast Reconstr Surg* 2013; **132**:61–9e.

42 Li XN, Qin Shu Q, Su JMF *et al.* Valproic acid induces growth arrest, apoptosis, and senescence in medulloblastomas by increasing histone hyperacetylation and regulating expression of p21Cip1, CDK4, and CMYC. *Mol Cancer Ther* 2005; **4**:1912–22.

43 Russell SB, Russell JD, Trupin KM *et al.* Epigenetically altered wound healing in keloid fibroblasts. *J Invest Dermatol* 2010; **130**:2489–96.

44 Ng Y-Z, Pourreyron C, Salas-Alanis JC *et al.* Fibroblast-derived dermal matrix drives development of aggressive cutaneous squamous cell carcinoma in patients with recessive dystrophic epidermolysis bullosa. *Cancer Res* 2012; **72**:3522–34.

45 Dees C, Schlottmann I, Funke R *et al.* The Wnt antagonists DKK1 and SFRP1 are downregulated by promoter hypermethylation in systemic sclerosis. *Ann Rheum Dis* 2014; **73**:1232–9.

46 Zhao X, Psarianos P, Ghoraie LS *et al.* Metabolic regulation of dermal fibroblasts contributes to skin extracellular matrix homeostasis and fibrosis. *Nat Metab* 2019; **1**:147–57.

47 Pellettier J, Thomas G, Volarević S. Ribosome biogenesis in cancer: new players and therapeutic avenues. *Nat Rev Cancer* 2018; **18**:51–63.

48 Wawruszak A, Halasa M, Okon E *et al.* Valproic acid and breast cancer: state of the art in 2021. *Cancers* 2021; **13**:3409.

49 Duenas-Gonzalez A, Candelaria M, Perez-Plascencia C *et al.* Valproic acid as epigenetic cancer drug: preclinical, clinical and transcriptional effects on solid tumors. *Cancer Treat Rev* 2008; **34**:206–22.

50 Pastar I, Marjanovic J, Stone RC *et al.* Epigenetic regulation of cellular functions in wound healing. *Exp Dermatol* 2021; **30**:1073–89.

51 Levra Levron C, Watanabe M, Proserpio V *et al.* Tissue memory relies on stem cell priming in distal undamaged areas. *Nat Cell Biol* 2023; **25**:740–53.

52 Nyström A, Bruckner-Tuderman L. Injury- and inflammation-driven skin fibrosis: the paradigm of epidermolysis bullosa. *Matrix Biol* 2018; **68–69**:547–60.

53 Watts C. The endosome–lysosome pathway and information generation in the immune system. *Biochim Biophys Acta* 2012; **1824**:14–21.

54 Li Q, Qin Z, Nie F *et al.* Metabolic reprogramming in keloid fibroblasts: aerobic glycolysis and a novel therapeutic strategy. *Biochem Biophys Res Commun* 2018; **496**:641–7.

55 Henderson J, Duffy L, Stratton R *et al.* Metabolic reprogramming of glycolysis and glutamine metabolism are key events in myofibroblast transition in systemic sclerosis pathogenesis. *J Cell Mol Med* 2020; **24**:14026–38.

56 Vincent AS, Phan TT, Mukhopadhyay A *et al.* Human skin keloid fibroblasts display bioenergetics of cancer cells. *J Invest Dermatol* 2008; **128**:702–9.

57 Xie N, Tan Z, Banerjee S *et al.* Glycolytic reprogramming in myofibroblast differentiation and lung fibrosis. *Am J Respir Crit Care Med* 2015; **192**:1462–74.